DOI: 10.21062/mft.2024.097 http://www.journalmt.com

Effect of Heat Treatment and Corrosion Load on the Microstructure of the Ti6Al4V Alloy

Roman Horký (0000-0002-4451-3006), Sylvia Kuśmierczak (0000-0002-5135-4170), Nataša Náprstková (0000-0003-4433-0581), Iryna Kambarová (0000-0003-3942-2481)
Faculty of Mechanical Engineering, J. E. Purkyne University in Usti nad Labem. Pasteurova 3334/7, 400 01 Usti nad Labem. Czech Republic. E-mail: sylvia.kusmierczak@ujep.cz, iryna.hren@ujep.cz, rohouni@mail.com, natasa.naprstkova@ujep.cz

In terms of mechanical, physical and chemical properties, titanium alloys are an important structural material for all branches of industry. One of the most important titanium alloys is the Ti6Al4V alloy. When performing operations associated with long-term heating of workpieces and parts made of titanium alloys in an air atmosphere, a layer of TiO_2 is formed on the surface of the product. Ti6Al4V alloy, also known as Ti64, is a two-phase α+β solid solution alloy in terms of microstructure, which has excellent corrosion resistance and biocompatibility. Through heat treatment, we can improve the mechanical properties of the alloy, improve the fracture toughness, influence and reduce the internal stress and influence the machinability of the material. Surface treatments of alloys by applying micro and nano layers of material are also important, which serve to extend the life of products made of this alloy or to improve the properties of the alloy. In the article, we analyze the effect of heat treatment at temperatures of 650 °C and 800 °C and corrosion load with salt fog in the range of 168 to 720 hours on the microstructure and microhardness of the Ti6Al4V alloy.

Keywords: Ti6Al4V, Microstructure, SEM and EDS analysis, Microhardness, Corrosion loads

1 Introduction

For the present time, titanium alloys are an important construction material due to their excellent physical and chemical properties. They are characterized by high strength, good plasticity, corrosion resistance exceeding that of stainless steels in seawater and a variety of corrosive environments, and other valuable properties. Due to the polymorphism and martensitic transformation that occurs during accelerated cooling, a two-phase titanium alloy is formed, which can be effectively hardened by heat treatment. Gases, namely oxygen, hydrogen and nitrogen, are absorbed when titanium and its alloys are heated, which is why a gas-saturated layer with the structure of an interstitial solid solution is formed. Inclusions of these compounds significantly increase the hardness and sharply reduce the impact strength and ability to plastic deformation [1]. If we expose titanium alloy parts to long-term exposure to heat in the air, a TiO_2 layer forms on the surface. For hot-processed components, the TiO_2 layer does not exceed 50-70 μm [2]. Layers saturated with oxygen are called alphated, as oxygen stabilizes the α-phase in titanium [1, 3,4].

The Ti6Al4V alloy, referred to as Ti64, or commercially Ti GR.5, is an α+β titanium alloy with low density, high strength, excellent corrosion resistance, and its biocompatibility is also important [1,2]. The Ti6Al4V alloy was initially intended to serve as a structural material for application in the aerospace industry for aircraft construction. Due to its low weight and high strength, its application was predestined for jet engines, gas turbines and many aircraft components [3-7]. For the aerospace industry, the Ti6Al4V alloy is constantly important, which also corresponds to the demand for it [5-8], other application areas in which these alloys are used are the automotive, chemical, marine, energy and biomedical industries. High strength, low density, high corrosion resistance and biocompatibility are valued properties of the Ti6Al4V alloy for use as a material for bridges and implants [2,9-13]. It is the most widespread and most produced titanium alloy ever, which finds its application in all areas of human industry, through products of common use, such as glasses, to body implants used in the field of biomedicine or the aviation industry [22-24]. More than 50 % of the world's titanium production is represented by this alloy [25-27]. This alloy is easily hardenable, malleable and easily weldable in the presence of an inert gas or vacuum. In addition, the alloy does not cause any reactions with body tissue in the human organism [28,29] and due to the formation of a protective TiO_2 coating, its high corrosion resistance is ensured [30,31].

Due to its high corrosion resistance to most corrosive acids and alkalis, its application to the marine

and chemical industries has rapidly expanded [2,14-15]. I confirm these results in my study by Klimas et al. [17] where they found that the action of Ringer's acid resulted in fragmentation of the structure and the formation of dendrites. These changes improved corrosion resistance and increased microhardness. There were no changes in the composition of the phases.

Through heat treatment in the presence of the surrounding atmosphere, a few nanometers thick and stable TiO_2 surface layer is gradually formed on the surface of the Ti-6Al-4V alloy. Depending on the processing temperature, the resulting surface layer structure can have three allotropic modifications. Namely rutile, brookite or anatase. During thermal oxidation, the surface morphology gradually changes from a thin adhesive layer to a thicker crystal layer with grains oriented towards the surface. The thickness of the layer increases with increasing temperature and duration of oxidation. The mechanical values of the surface also increase in proportion to it, thus also the corrosion resistance. As can be read from a number of professional articles, the most frequently used processing temperatures range from 500 to 800 °C, while the duration of processing at these temperatures ranges from 1 to 60 hours. Garcia-Alonso et al. [18] state in their work that after only one hour there is a visible influence on the mechanical properties and an improvement in corrosion resistance. The mentioned temperatures are used in an attempt to influence corrosion resistance, suitable especially because it is possible to guarantee the formation of an oxide layer with a predominant rutile morphology [17-21].

The aim of the presented article is to analyze the effect of heat treatment at temperatures 650 °C and 800 °C and salt spray corrosion load in the range of 168 to 720 hours on the microstructure and microhardness of the Ti6Al4V alloy.

2 Experimental material and methodology

For experimental purposes, 10 samples of the Ti-6Al-4V alloy were used, which were prepared from a rolled rod with a diameter of 12 mm with the chemical composition: Al-6.25 wt. %, C-0.08 wt.%, Fe-0.25 wt.%, V-4.01 wt.%, H-0.015 wt.%, N-0.05 wt.%, O-0.2 wt.% . The material was processed and then cut into cylinders of the same size: length – 30 mm and diameter – 10 mm (Fig. 1).

For the experiment, two samples were left without any modifications and the other eight samples were heat treated. Specifically, the samples were annealed at 650 and 800°C for 2 hours. Subsequently, the samples were left inside the furnace until they were completely cooled. The next process was the corrosion load of such heat-treated samples. The corrosion load was carried out in accordance with the ČSN EN ISO 9227 standard [32]. The prepared samples were placed in the LIEBISCH corrosion chamber, where they were in an environment of salt fog, formed by a NaCl solution. The duration of the corrosion load in the salt fog was 168, 240, 480 and 720 hours, at a maintained temperature of 35 °C.

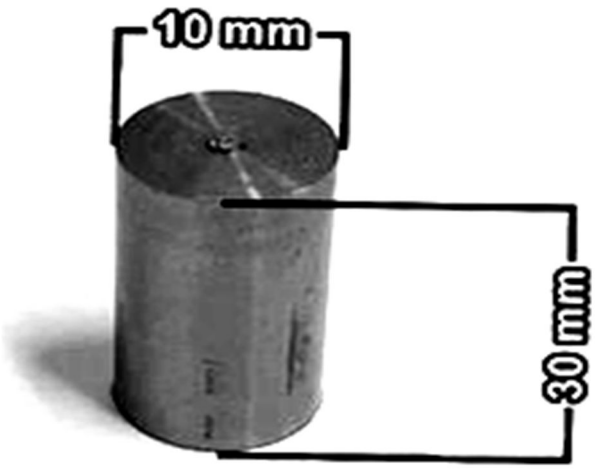

Fig. 1 *Sample of offcuts from titanium rod*

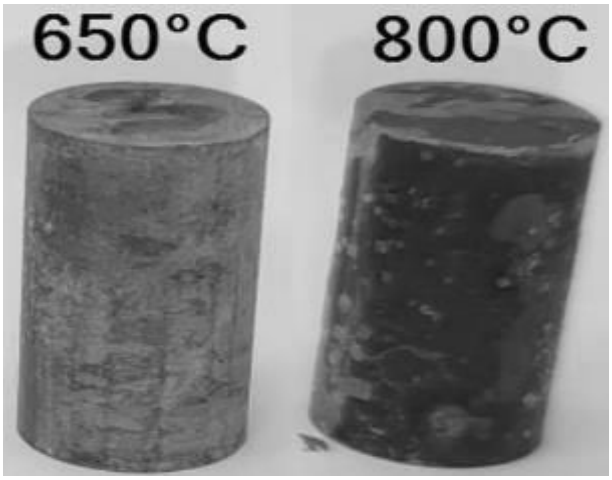

Fig. 2 *Surface condition of heat-treated samples*

For the analysis of the microstructure of the layer and the base material, 10 samples were metallographically prepared - by wet grinding and then polishing with diamond emulsions from Struers. The last mechanical-chemical treatment was carried out using an Al_2O_3 suspension with a grain size of 0.3 μm. After etching with a mixture of nitric and hydrofluoric acids (Kroll etchant), the structures of the material were observed using light microscopy on a confocal laser microscope LEXT OLS 5000 from Olympus.

The microhardness test of all samples was performed in accordance with the ČSN EN ISO 6507-1 standard on the FUTURE-Tech FM-300 device. A 136° diamond indenter creating a square indentation was used to measure the microhardness. The load value established a HV of 0.01 (F = 0.098 N, 10 g), which acted on the test specimen for 10 s. Due to the thickness of the layer, emphasis was placed on the selected diagonal of the indenter in order to comply with the ISO 6507-1 standard.

From a number of professional articles dealing with the formation of a surface oxide layer as a result of thermal oxidation, it can be read that its gradual growth can already be observed from 500 °C onwards. At lower processing temperatures, as a rule, lower thicknesses are achieved, but higher compactness and better adhesion. Higher temperatures (800 °C and more) can ensure the formation of a stronger surface layer, which provides higher values of selected mechanical properties, but if the conditions of the entire process are incorrectly chosen, there is a risk of worse adhesion of this crystalline layer. For these reasons, temperatures that cover the entire mentioned range were chosen for the experiment.

By simply visual observation of the heat-treated samples (see Fig. 2), quite significant surface coloration was detected.

In the case of titanium and its alloys, the change in color after heat treatment is usually associated with a change in the thickness of the surface oxide layer and with a change in the interference of incident light radiation. Depending on the heat treatment temperature and subjecting the samples to a corrosive environment, the prepared samples had the markings shown in tab. 1.

Tab. 1 *Marking of samples depending on heat treatment and corrosion load*

Heat treatment [°C] / Corrosion loads [hours]	Without load	168	240	480	720
0	A	-	-	-	-
650	B	B1	B2	B3	B4
800	C	C1	C2	C3	C4

3 Evaluation of surface layer thickness

In the first part of the experiment, a microscopic analysis of the thickness of the surface layer was performed using a Vega Tescan 3 electron microscope with a Bruker analyzer. Fig. 3 shows a reference sample that was not subjected to corrosion.

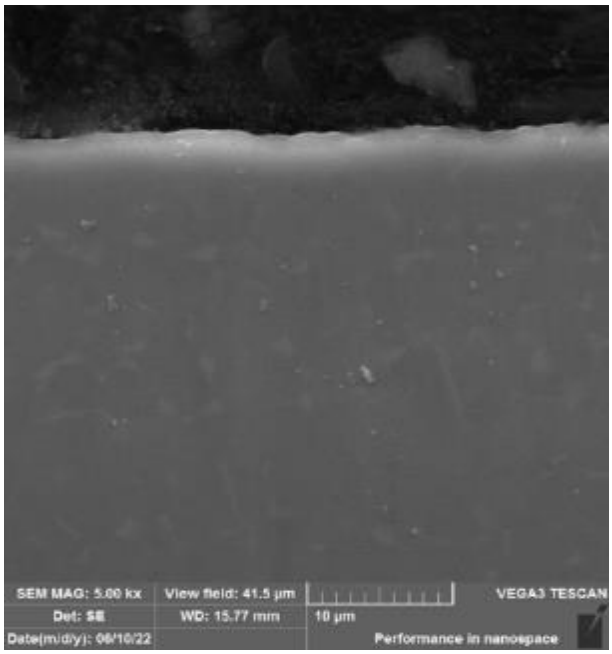

Fig. 3 *The thickness of the surface layer of samples A*

For samples of set B, which were heat treated at a temperature of 650 °C. For this set of samples, the material was affected to a depth of approximately 1-2 µm from the surface, see Fig. 4, 5. An even and homogeneous layer was achieved for all samples, which even after 720 hours of corrosion load showed signs of integrity, smooth and stable connection with the underlying material and no obvious signs of damage were recorded, Fig. 4 – 7.

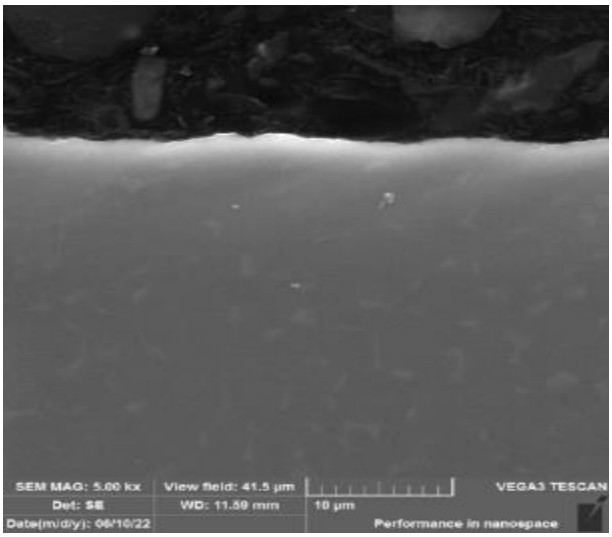

Fig. 4 *The thickness of the surface layer of samples B1 - 650°C*

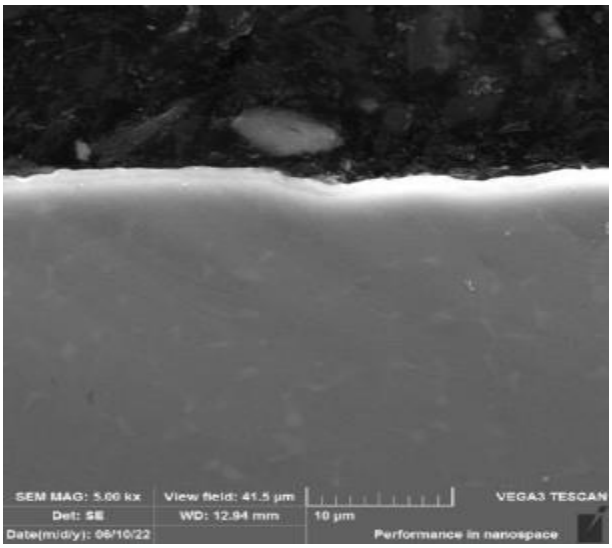

Fig. 5 *The thickness of the surface layer of samples B2 - 650°C*

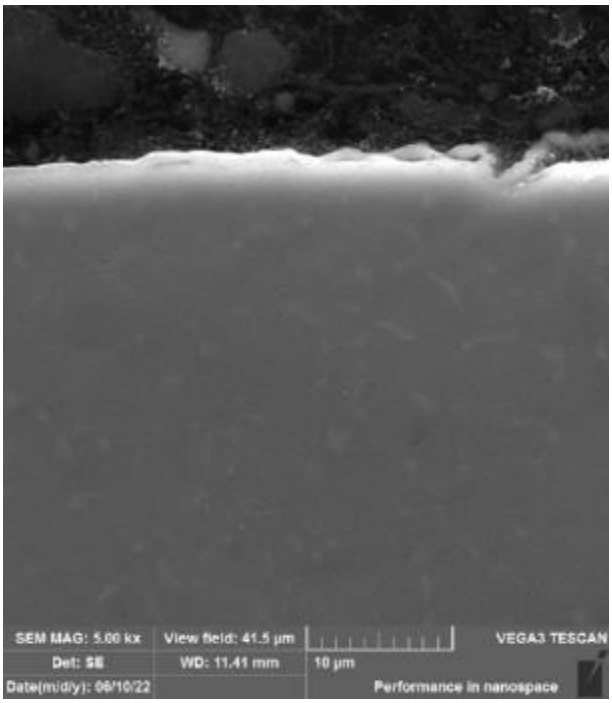

Fig. 6 *The thickness of the surface layer of samples B3 - 650°C*

From the point of view of elemental mapping, Fig. 8 to 11, in the case of oxygen, we can talk about obtaining an approximately 2 µm thick oxide layer, which shows signs of compactness, regular arrangement and adhesion to the substrate even after a period of 720 hours, during which the sample was exposed to a corrosion load.

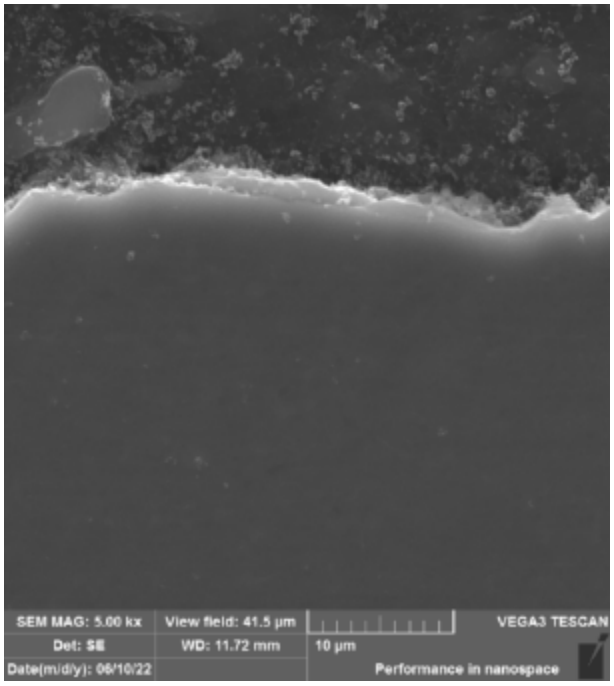

Fig. 7 *The thickness of the surface layer of samples B4 - 650°C*

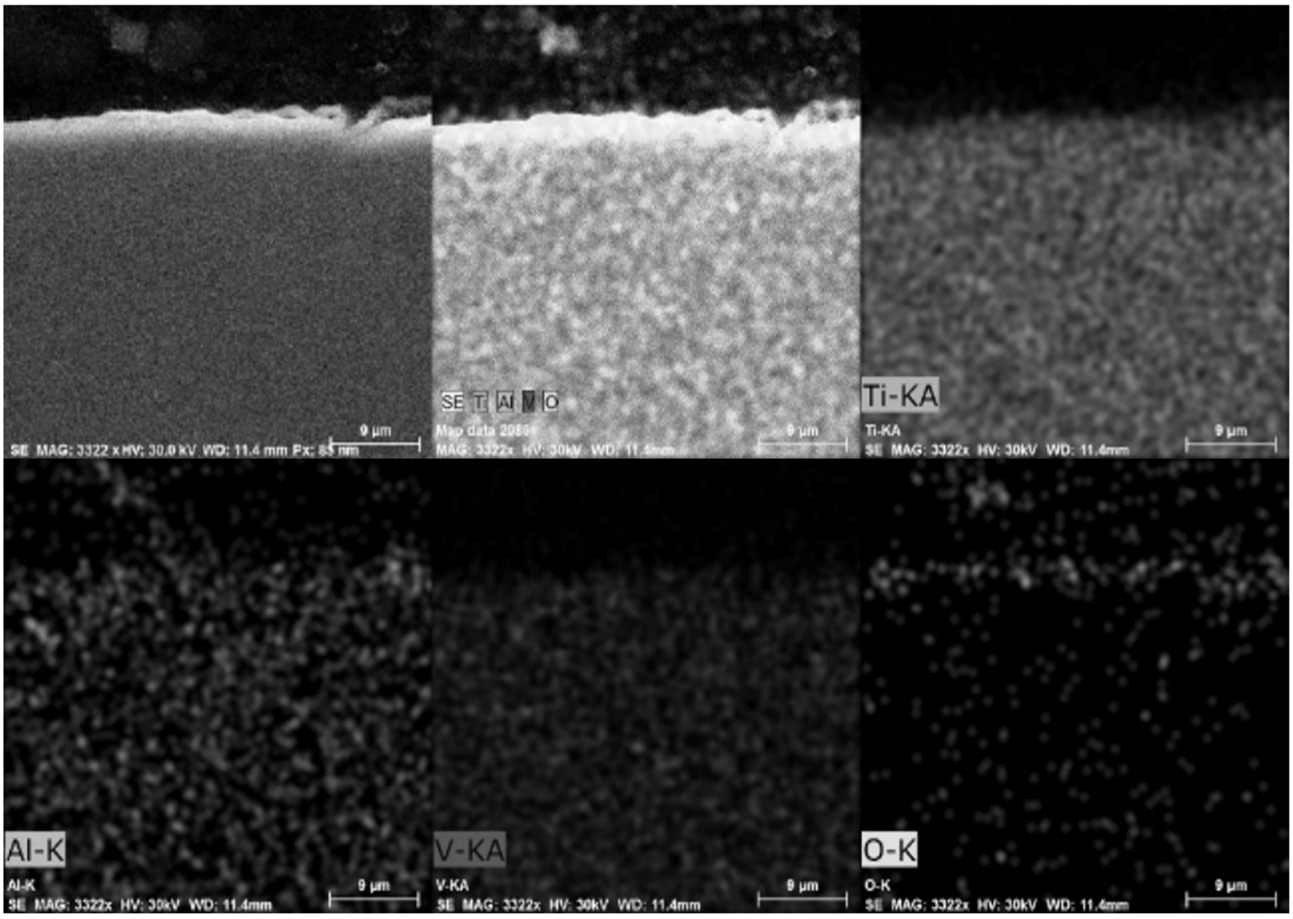

Fig. 8 *Mapping from the example B1*

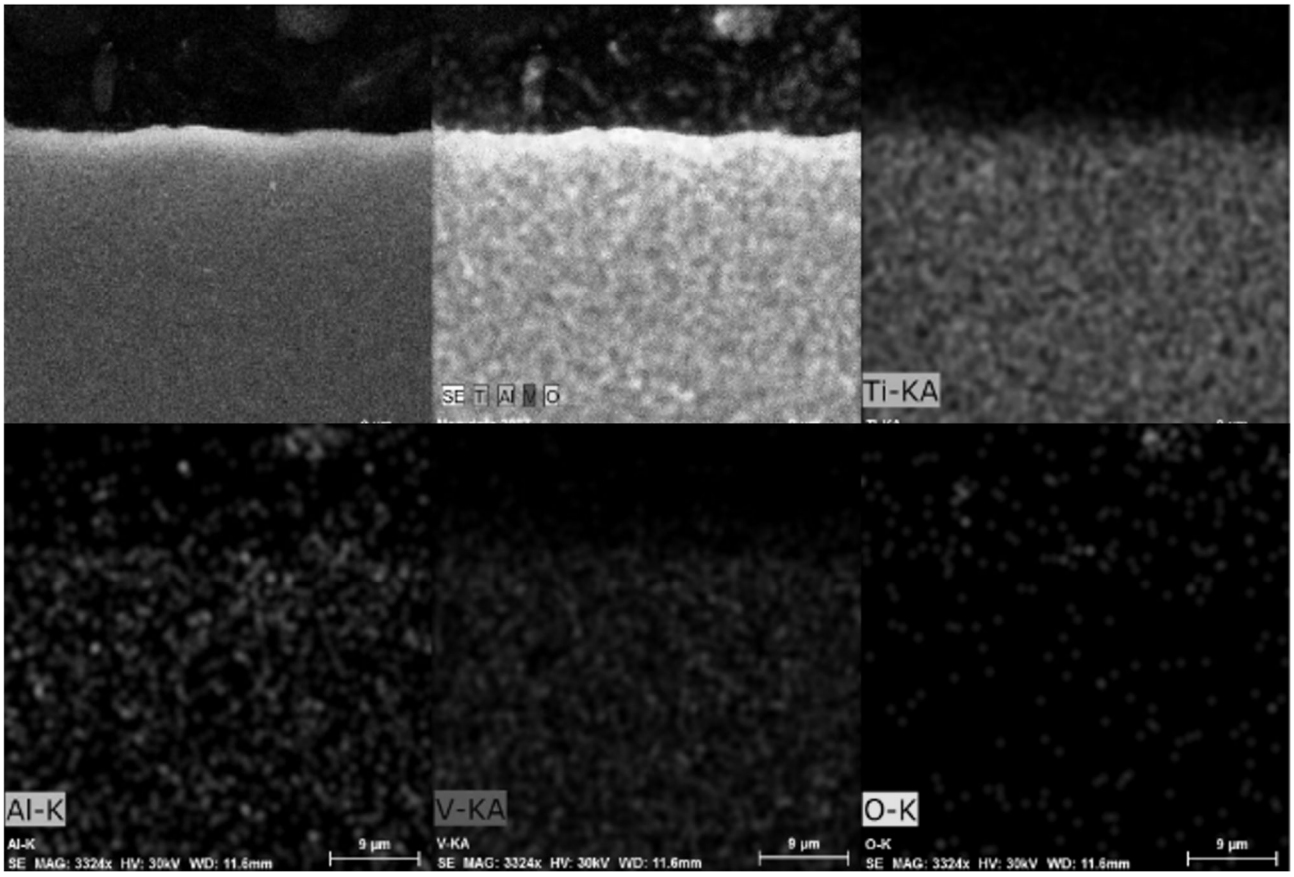

Fig. 9 *Mapping from the example B2*

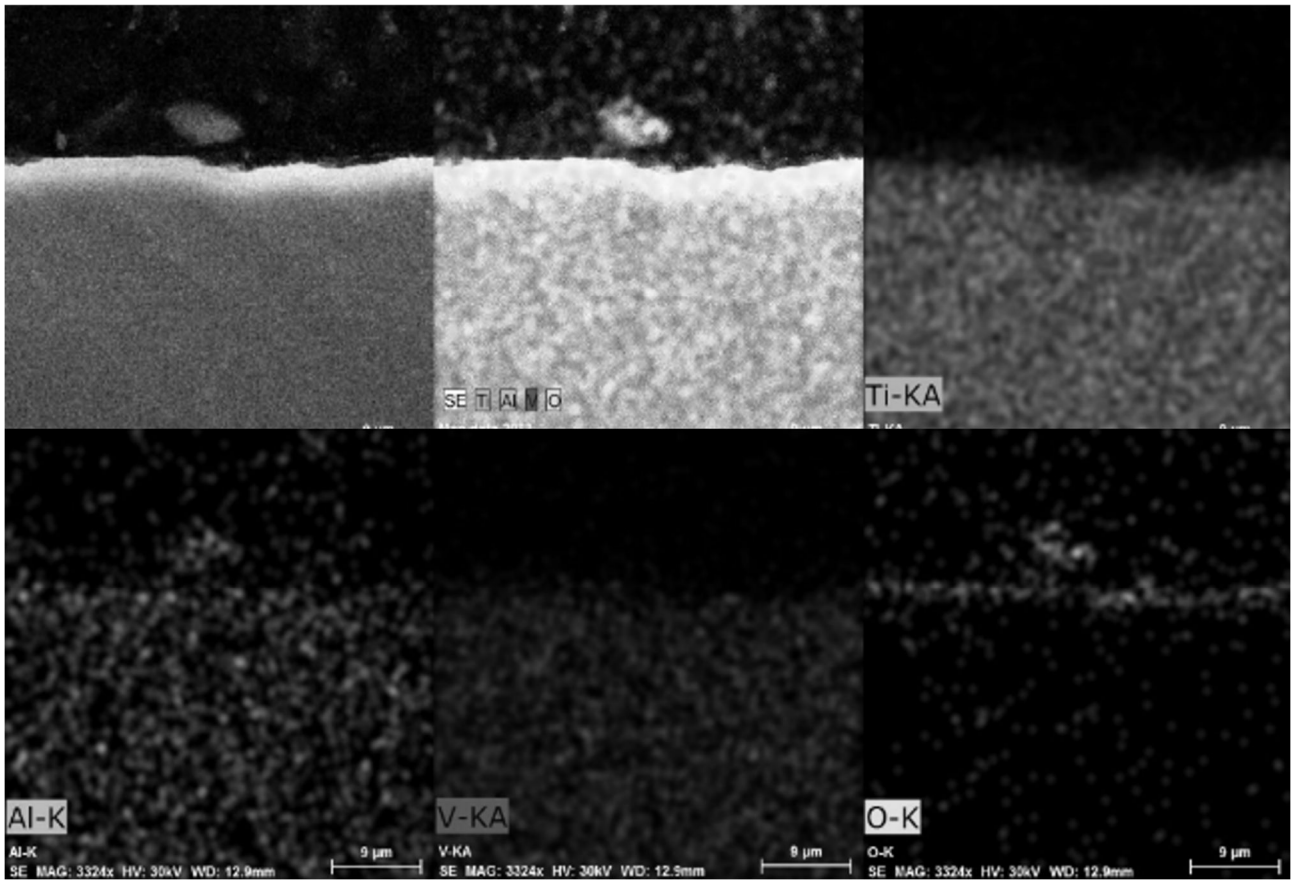

Fig. 10 *Mapping from the example B3*

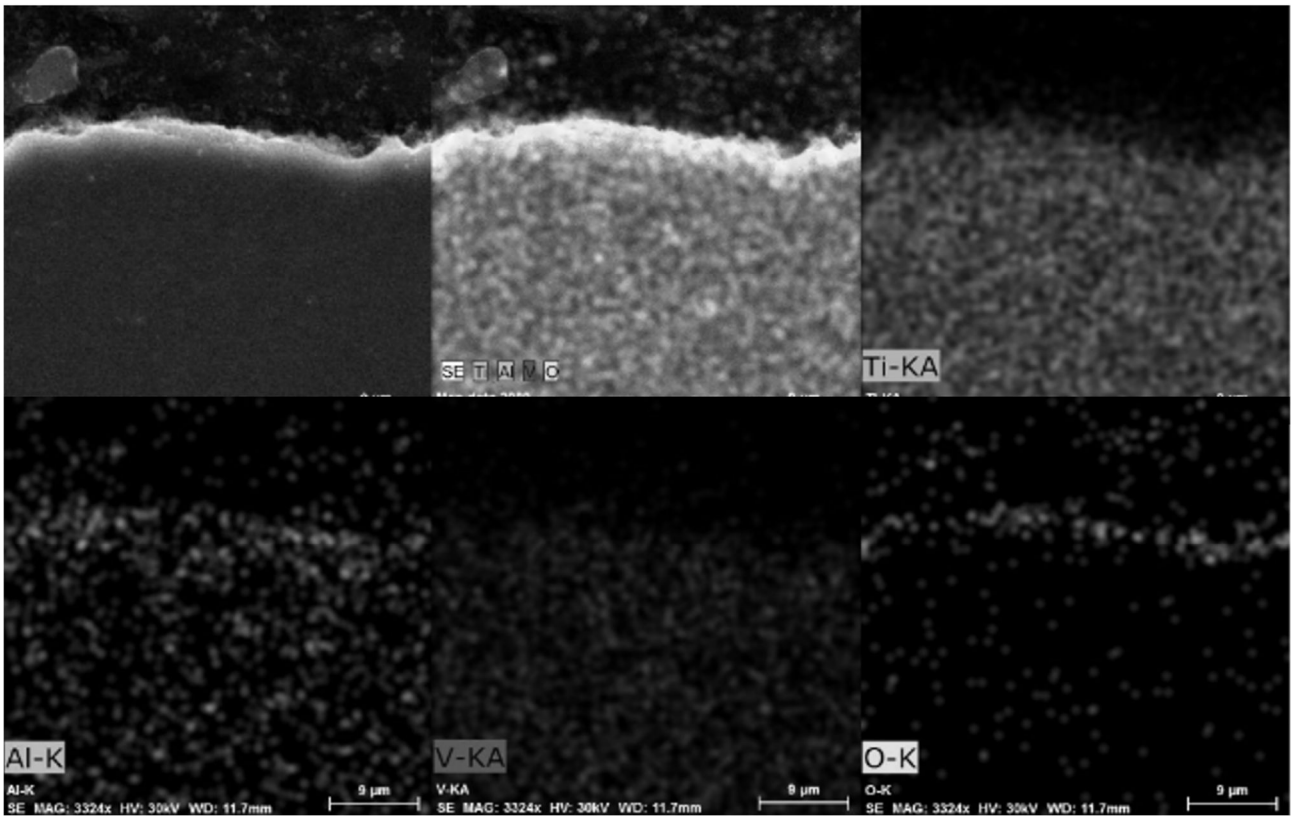

Fig. 11 *Mapping from the example B4*

The first changes in the layout, from the point of view of the remaining elements, begin to appear with aluminum. From the pictures it is possible to see that due to the heat treatment aluminum starts to diffuse, which starts to concentrate under the surface of the sample. This process is most clearly visible on the image of sample B4, shown in Fig. 11.

4 Evaluation of surface layer thickness

The set marked as C1-C4 represented the second evaluated set of samples, which was heat-treated at a temperature of 800 °C, i.e. at a temperature which, according to the research of expert articles, supports the intensive formation of a surface oxide layer, which, however, can lead to separation from the underlying substrate. Images of the resulting layer are shown in Fig. 12-15.

As can be seen from the above images, the temperature of 800 °C and the processing time of 2 hours really promoted the intensive growth of the surface oxide layer, Fig. 12-15. As a result of the heat treatment, a surface layer with a thickness of about 30 µm was formed, which is more than ten times the thickness compared to the layers obtained with previous sets. However, despite the use of the onset temperature curve, which was chosen on the basis of an expert article (D.S.R. Kryshna [34]), such a layer was not formed that would be perfectly connected to the underlying substrate, and it can therefore be assumed that during the tear adhesion test, which is in also mentioned in the above article, the upper part of the surface layer would be separated from the rest of the material. This statement is based mainly on the behavior of sample C2, whose image is also shown in Fig. (13), and in which spontaneous separation of part of the surface layer occurred, which can be seen in detail in Fig. 16. Compared to the remaining samples, it is possible to see here the resulting average thickness of 17.78 µm with a standard deviation of 0.43 µm. On this sample, already after the heat treatment, cracks were visible to the naked eye, which evenly covered the entire surface of the test sample.

Figures 17 to 20 present elemental maps of samples heat treated at 800°C. As can be seen from the images, due to this temperature, a relatively significant surface layer of oxide was obtained compared to the previous variant. Oxygen can be seen on them not only in the entire extent of the newly formed surface layer, but also below it, where, as already mentioned, it dissolves in the basic matrix, thereby strengthening it. In addition to oxygen, it is also possible to observe a significant diffusion of aluminum in the surface layer, which already began to manifest itself with the previous set. In this case, however, its relatively significant accumulation was noted in the area below the surface, approximately to a depth of 2 to 3 µm.

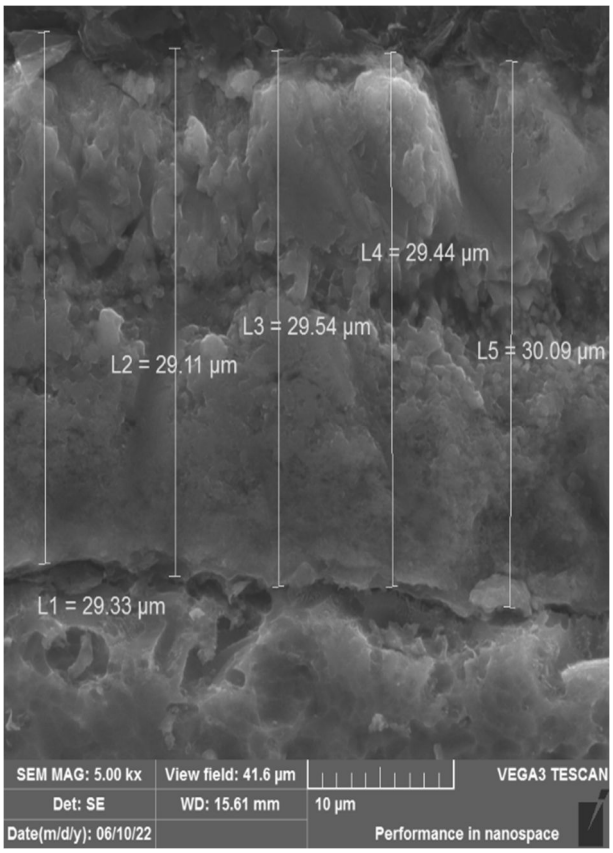

Fig. 12 *The thickness of the surface layer: sample C1 - 800 °C*

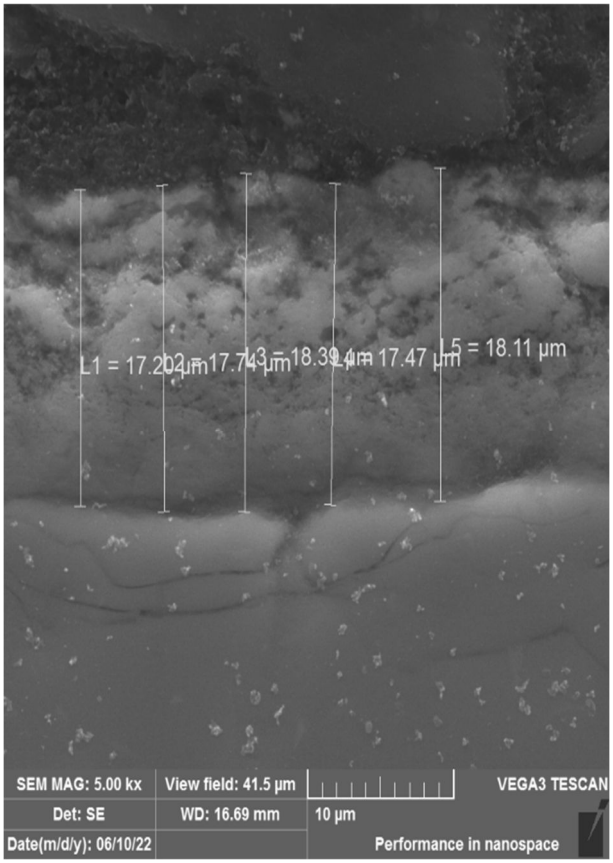

Fig. 13 *The thickness of the surface layer: sample C2 - 800 °C*

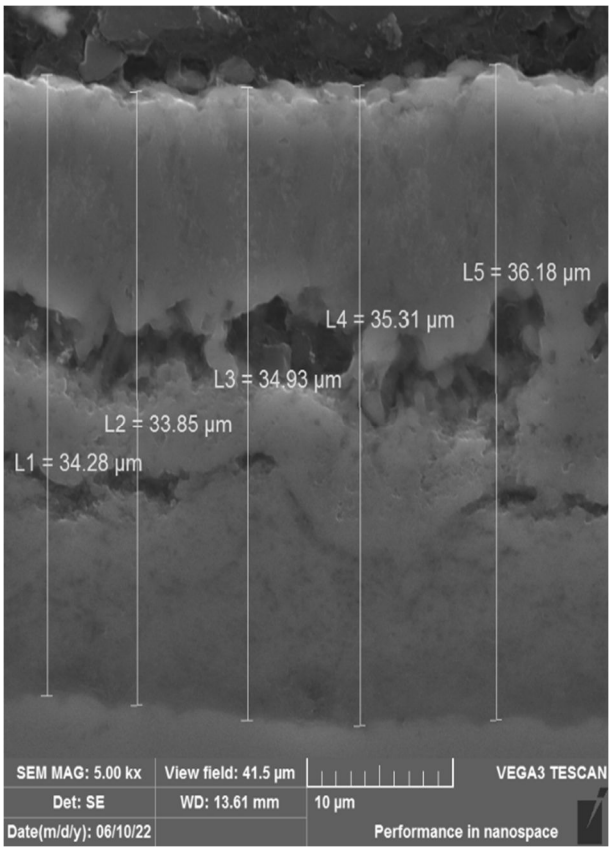

Fig. 14 *The thickness of the surface layer: sample C3 - 800 °C*

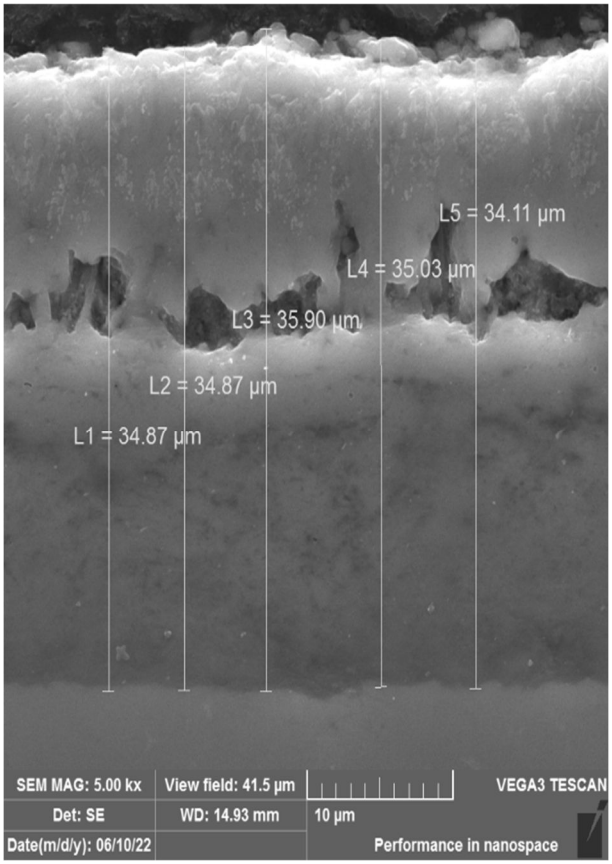

Fig. 15 *The thickness of the surface layer: sample C4 - 800 °C*

ISSN 1213–2489
e-ISSN 2787–9402

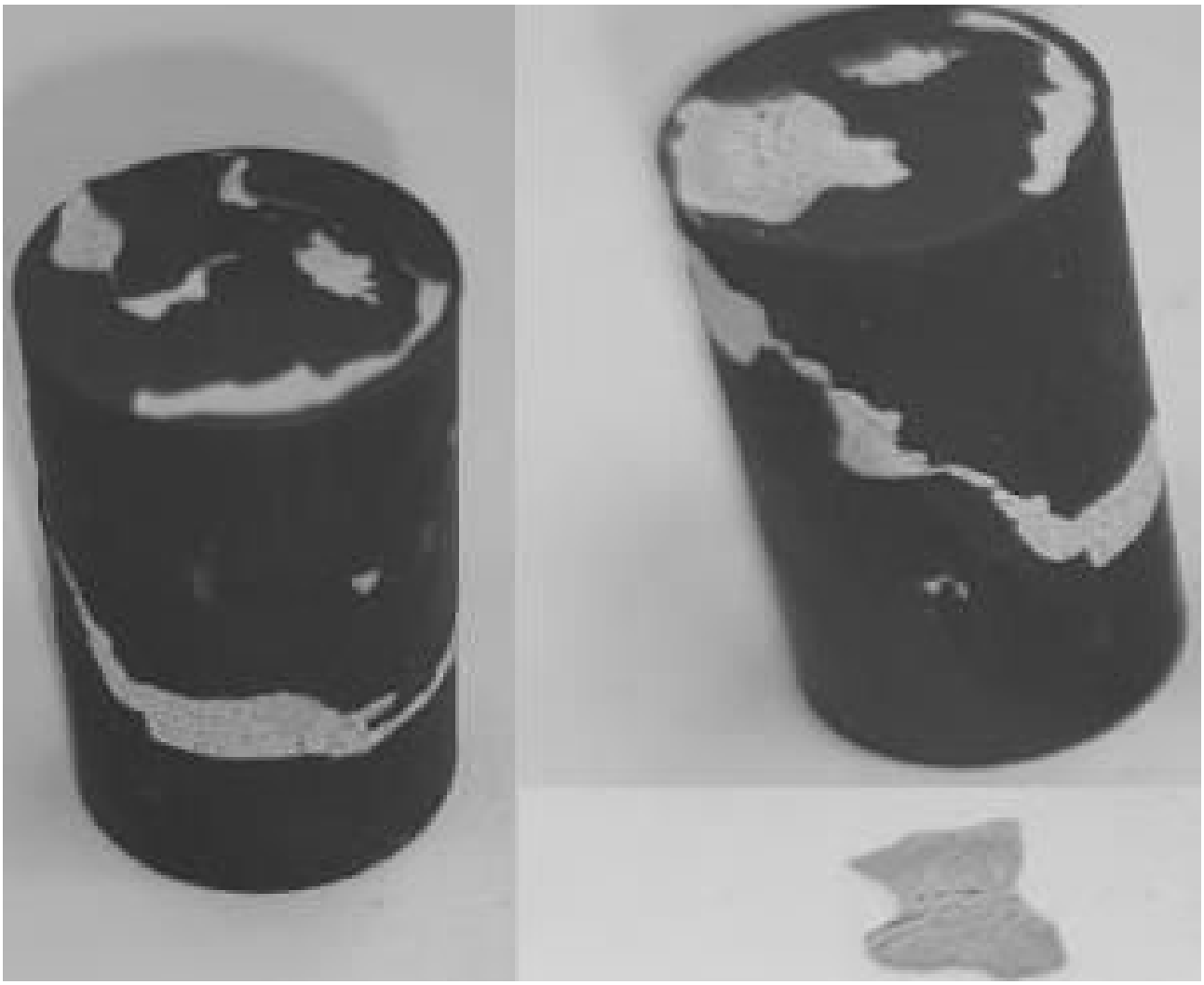

Fig. 16 *Peeling of the surface layer – sample C2*

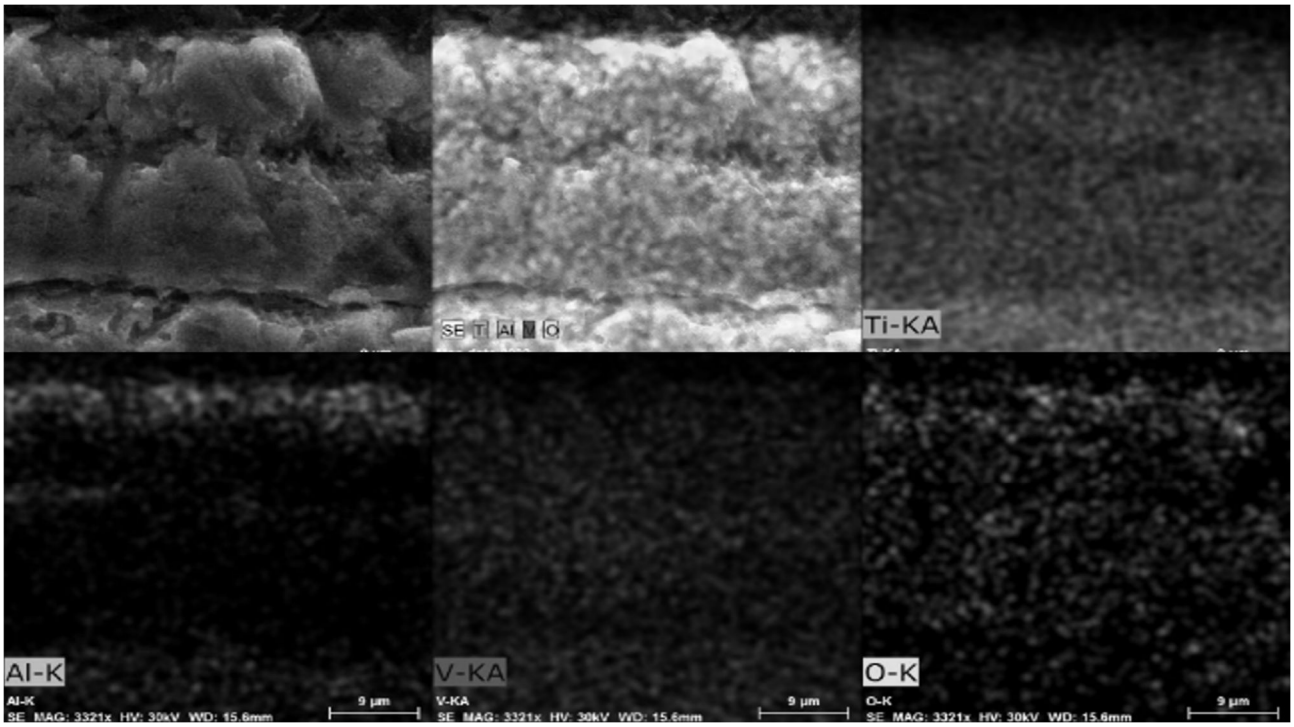

Fig. 17 *Mapping from the sample C1*

ISSN 1213–2489
e-ISSN 2787–9402

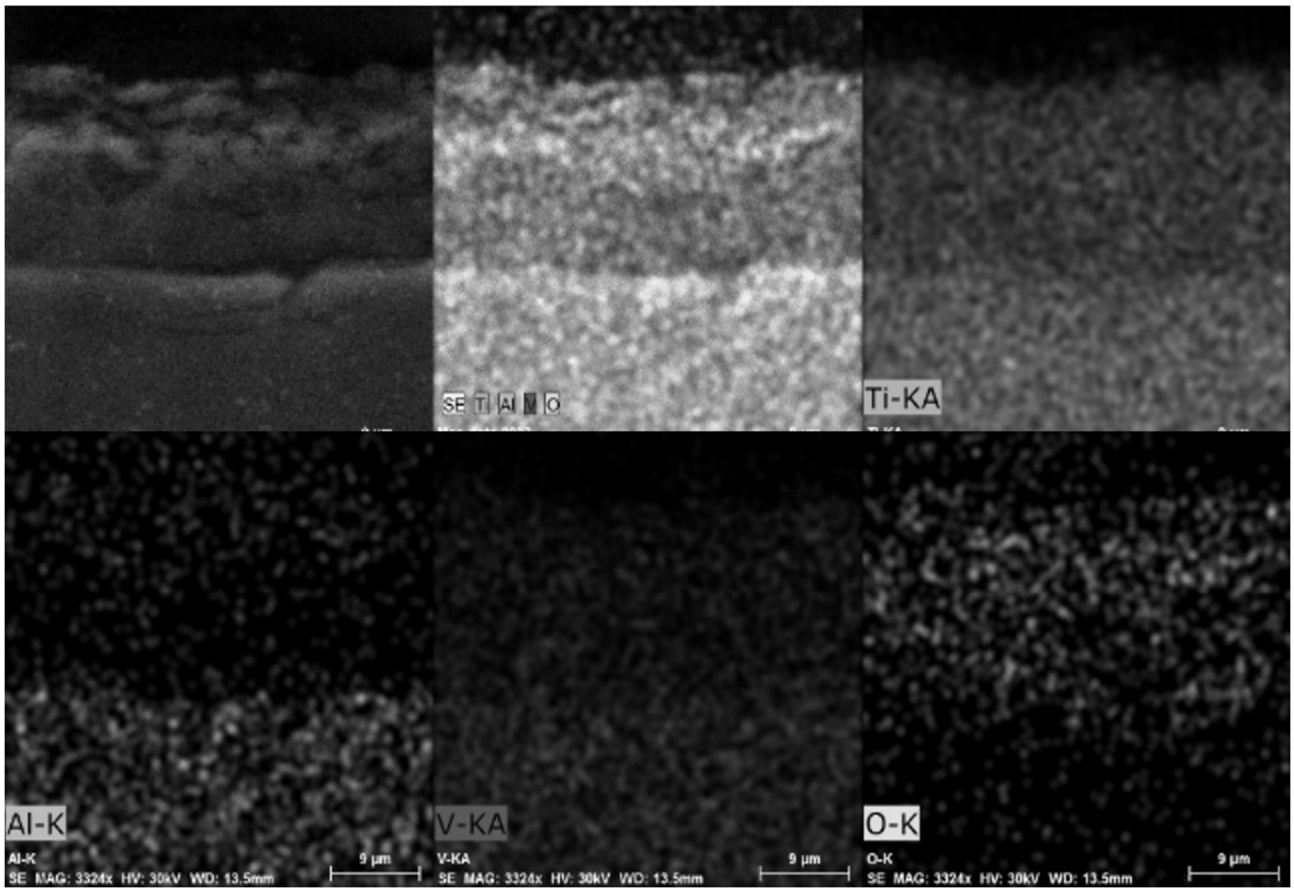

Fig. 18 *Mapping from the sample C2*

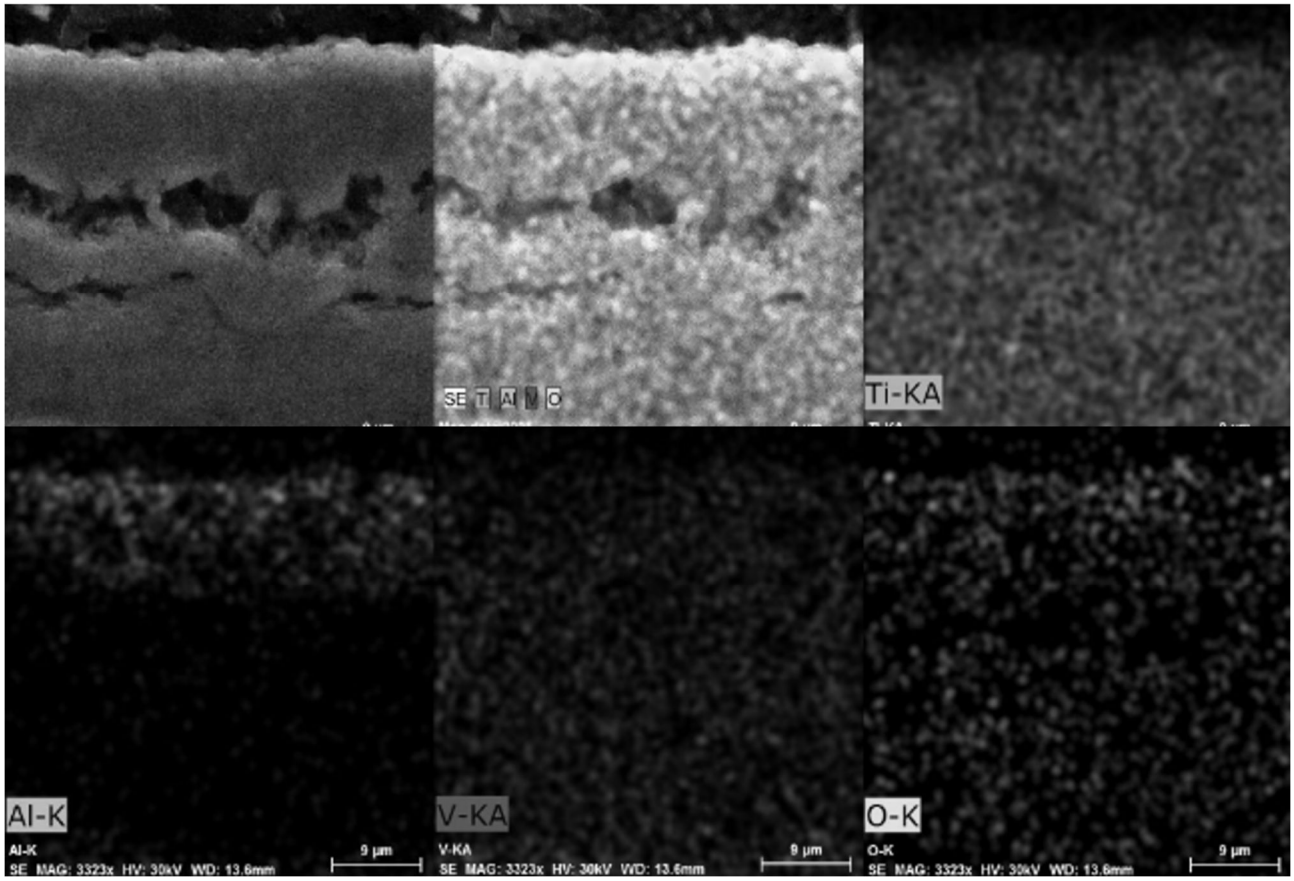

Fig. 19 *Mapping from the sample C3*

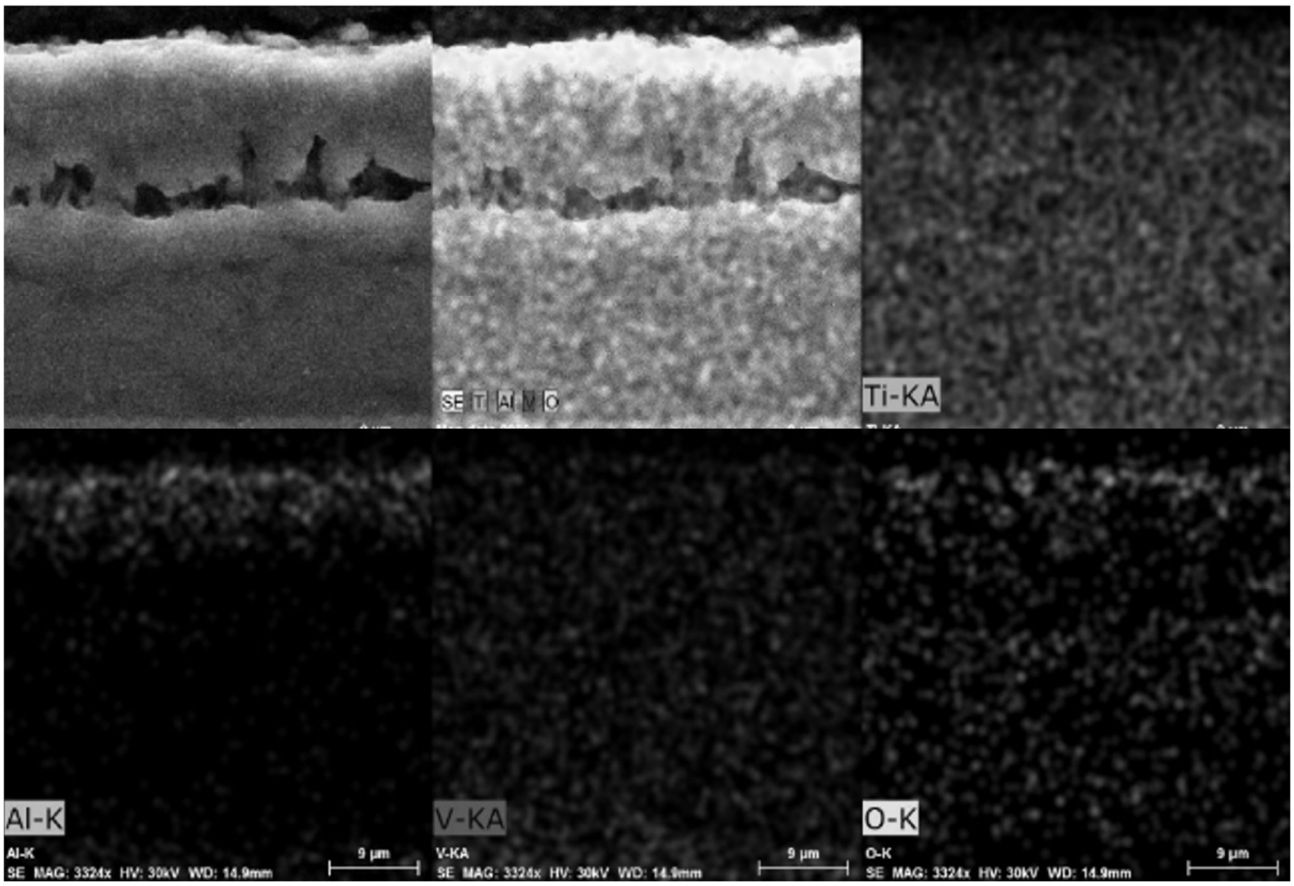

Fig. 20 *Mapping from the sample C4*

Furthermore, for the first time, changes in the distribution of vanadium were noted for this set. For sample C1, see Fig. 17, its incipient diffusion of this element into the surface layer is very clearly visible, which at higher concentrations of aluminum could lead to the formation of intermetallics, which are characterized by good corrosion resistance but high brittleness. At lower processing temperatures, no significant changes have yet been observed in the case of vanadium.

5 Evaluation of hardness according to CSN EN ISO 6507-1

The hardness of all samples was evaluated according to the ČSN EN ISO 6507-1 standard [35]. The research was conducted on a FUTURE-Tech FM-300. A 136° square indentation diamond indenter was used to measure microhardness, and the load value determined HV 0.01 (F = 0.098 N, 10 g). The duration of the load, which acted on the test body, was set at 10 s. The microhardness values of the reference sample A, i.e. the sample without heat treatment and corrosion load, are given in Tab. 2.

The graph below shows the measured microhardness values of sample sets B and C. Fig. 21 shows the values of the heat-treated sample B, which was not subjected to corrosion. Figure 22 shows the values of the samples that were first heat-treated under the same conditions and then subjected to a corrosion load.

The increase in hardness is caused by the breakdown of the martensitic structure, i.e., $\alpha' \rightarrow \alpha + \beta$. This happens because the martensite structure is not formed after heat treatment, the hardness increases during the aging process probably due to the precipitation of the fine α phase from the β phase, i.e., metastable $\beta \rightarrow$ fine $\alpha + \beta$ [35] Fig. 23 -25. The heat-treated structure showed microhardness values of around 350 HV compared to the unheated one, which set - 300 HV.

Tab. 2 *Microhardness of the sample A podle ČSN EN ISO 6507-1*

Distance [µm]	10	25	50	75	100	125	150
Average value	305.1	302.3	305.5	304.0	305.3	307.5	305.2
Standard deviation	3.9	1.8	1.7	3.1	0.8	1.1	2.5

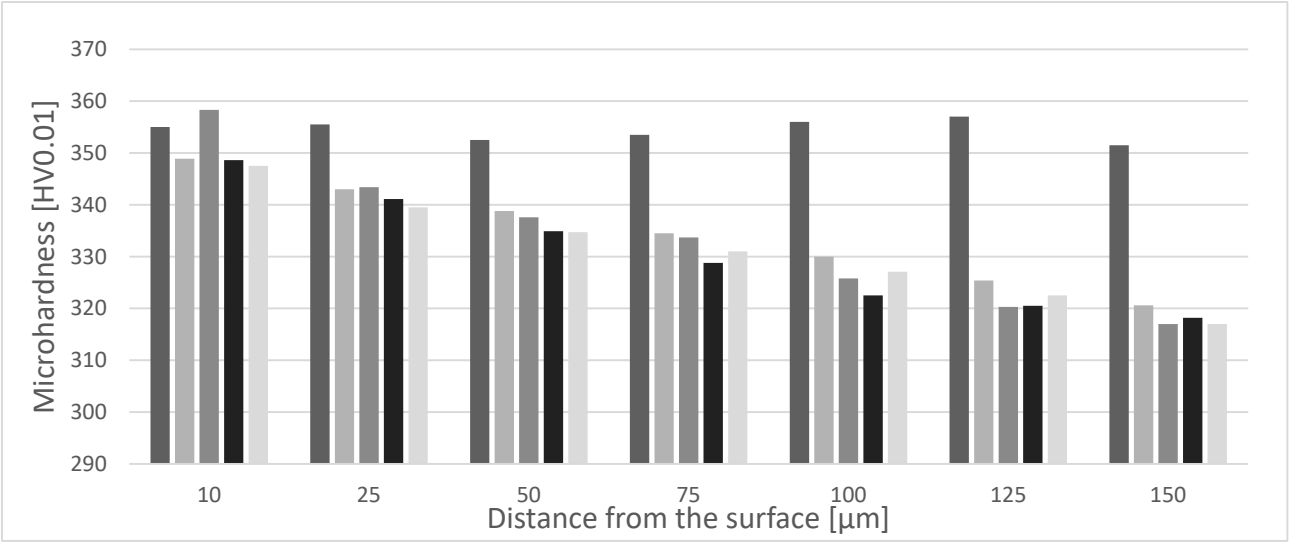

Fig. 21 *Average microhardness values of sample set B*

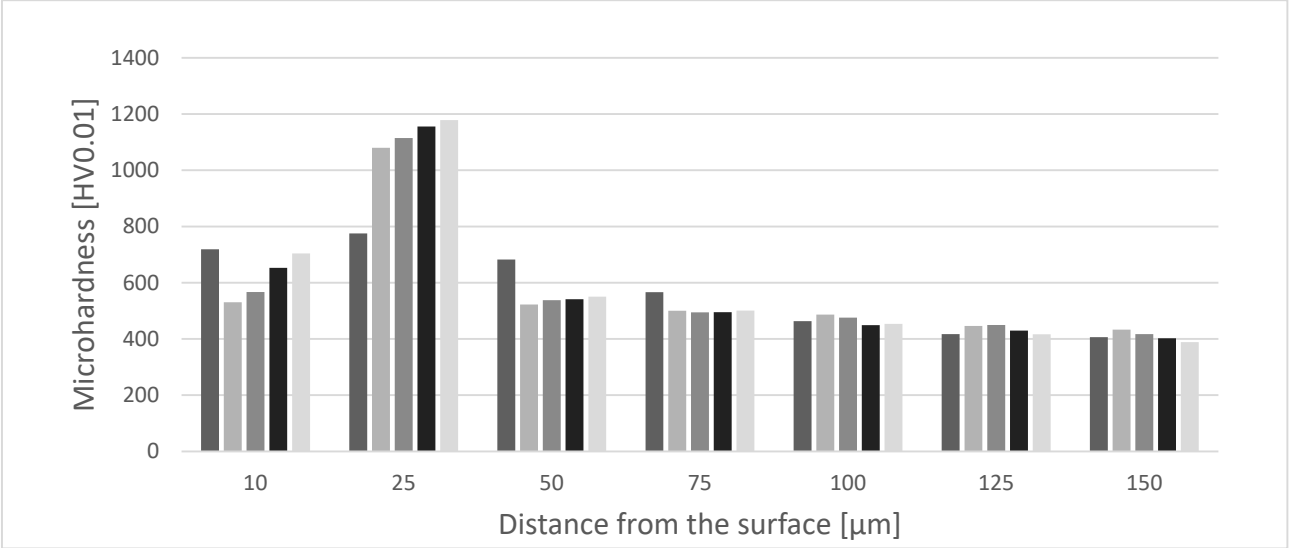

Fig. 22 *Average microhardness values of sample set C*

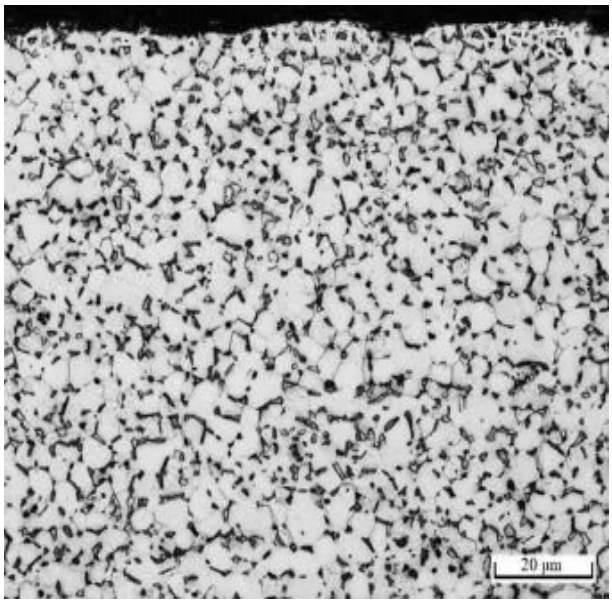

Fig. 23 *Microstructure sample A*

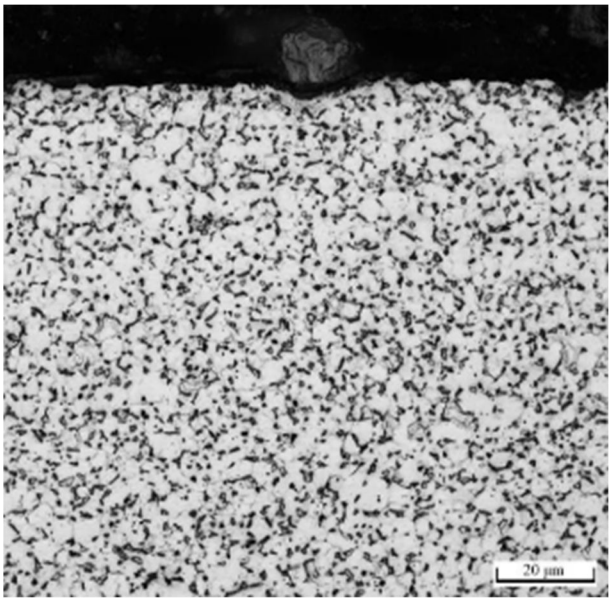

Fig. 24 *Microstructure sample B4*

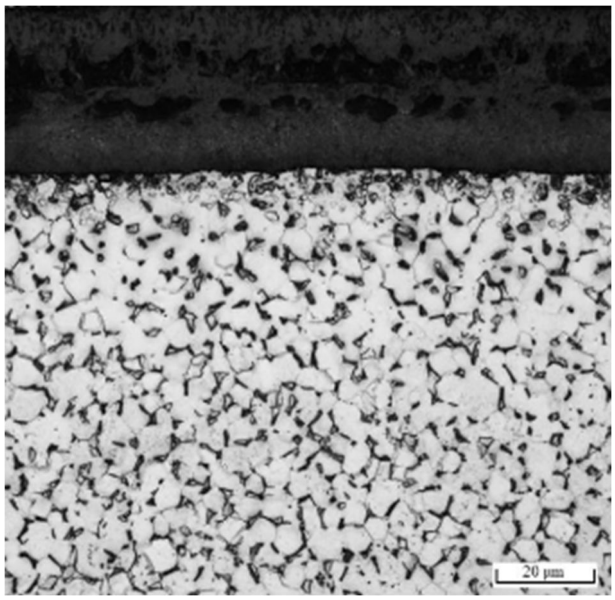

Fig. 25 *Microstructure sample C4*

From the top of the figure, it is possible to confirm the stated results for this variant, that heat treatment at 650 °C resulted in the formation of an oxide layer, which compared to reference sample A, caused an approximately 10% increase in hardness in the area just below the surface (10 μm) and an approximately 10% increase in the field of basic material. As can be seen further, as a result of the corrosion action, corrosion products began to form on the surface, which by their nature caused a further increase in hardness in close proximity to the surface. Here, a gradual increase can be seen depending on the length of the corrosion load, with the highest values being reached for sample B3. For sample B4, a decrease has already occurred due to damage and separation of the surface layer due to corrosion attack. When comparing the corrosion-stressed samples of this variant with sample B1, which was only heat-treated, it is possible to observe a slight decrease in microhardness. While the non-corroded sample shows fairly constant values with minimal variance, larger variances of the measured values are visible in the corroded samples. This dispersion can be attributed, as reported by Hasan Güleryüz [35] in his professional article, to the involvement of softer areas at greater depths of the tested sample. In contrast, the decrease in hardness can be attributed to a change in chemical composition due to aluminum diffusion, which was observed in the elemental maps. In the case of samples from set C, which obtained the largest thickness of the surface layer, there were also the most significant changes from the point of view of microhardness. From the presented results, a significant increase in hardness is visible in the area of the upper part of the surface layer and then in the area of the transition between the layer and the underlying material in the case of sample C1 without corrosion. On the contrary, a considerable decrease is visible in the middle part of the layer. However, the opposite trend is visible in the samples subjected to corrosion, which indicates both the interaction of the corrosion environment with diffused elements and, at the same time, the penetration of the corrosion environment into the defects in the middle part of the formed layer, where corrosion products are formed, which is manifested externally by a significant increase in hardness.

From the microhardness values, which were obtained from corrosion-stressed samples, and which were visualized in the following graph, the effect of corrosion on the heat-treated alloy is very clearly visible. As a result of the corrosion load, a visible decrease in hardness occurred just below the surface, i.e. in the area where the diffusion of aluminum and vanadium was observed on the elemental maps. This decrease occurred precisely as a result of the diffusion of the mentioned elements, which significantly changed the chemical composition of the given area, due to which there was a sudden change in corrosion resistance. However, with continued loading, a significant amount of hard corrosion products were formed, which began to form both on the surface and at the same time in the area with disturbed cohesion of the surface layer, which was visible in the previous chapter in Fig. 15. As a result, there was a jump in microhardness in this area, which increased by approx. 300 to 400 HV0.01 depending on the length of corrosion exposure.

6 Conclusion

In the mentioned article, an experiment was conducted that deals with the effect of heat treatment on selected properties of the Ti6Al4V alloy. During the experiment, two different heat treatment temperatures were used: 650 °C and 800 °C with cooling in a closed furnace. These samples were compared with non-heat treated samples. After that, the samples were subjected to a corrosion load for 168 to 720 hours.

The microstructure of the resulting samples did not show any striking differences. The only difference was the formation of compact TiO_2 layers. This phenomenon confirmed our expectations and we can focus on higher temperatures during heat treatment in the next work.

For samples heat-treated at 650 °C, a visible increase in thickness was observed both in the surface layer and in the oxygen diffusion zone, which was manifested by a significant increase in surface and subsurface hardness. For the samples heat-treated at 650 °C, due to the formation of hard oxides on the surface and the dissolution of oxygen below them, there was an increase in the hardness in the surface area compared to the unheated sample by an average value of approximately 85 HV0.01. At the same time, a slight decrease in hardness was possible, which occurred as a result of the incipient diffusion of aluminum.

However, in both cases, a positive effect of the heat treatment on the corrosion behavior was demonstrated due to the formation of a stable oxide layer, which is visible in the minimal differences between the samples loaded for 168 and 720 hours. For the samples processed at a temperature of 650 °C and loaded for 720 hours, the smallest dispersion of the measured values of microhardness was also recorded, which also indicates the increased stability of the formed oxide layer. At these temperatures, no significant changes in the microstructure were also noted, which means that the equiaxed α+β structure was preserved in both cases.

In contrast, the temperature of 800 °C contributed, compared to lower processing temperatures, to the formation of a very pronounced surface layer, the thickness of which was around 30 μm. This temperature also caused visible changes from the point of view of the microstructure, where a greater content of the β phase was obtained in the structure, due to the diffusion of aluminum as a stabilizer of the alpha phase into the surface layer. As a result of the diffusion of aluminum into the surface layer, the formation of Al_2O_3 can also be assumed at the interface between air and oxide, which, according to some expert articles, acts as a barrier and causes a decrease in the amount of dissolved oxygen under the oxide layer.

Despite the use of the start-up temperature curve, which was expected to have a positive effect on obtaining a homogeneous layer with good adhesion to the substrate, it was not possible to support the growth of a defect-free layer. Defects were noted on all samples, which had a very significant effect on the corrosion behavior itself, as the corrosion environment penetrated these defects and subsequently separated part of the layer. The formation of corrosion products in the place of defects is also very visible on the measured values of microhardness, where there is a sudden increase of 300 to 400 HV0.01.

From the point of view of the influence of heat treatment on corrosion behavior and microstructure, it is therefore possible to say that the temperature of 650 °C proved to be more unfavorable in this experiment. At this temperature, a homogeneous and perfectly adherent oxide layer was achieved, where no defects were visible and it was not damaged even as a result of corrosion stress. This layer, together with the oxygen diffusion area, contributed to an increase in hardness not only in the surface but also in the subsurface layer, while the average value of this increase was around 80 HV0.01 in the surface and around 50 HV0.01 in the subsurface layer. No changes in the microstructure of the base material were also noted at this temperature. After heat treatment and corrosion stress, the equiaxed α+β structure with a uniform and regular distribution of both phases was still preserved. Such a structure is characterized by relatively high stability, strength and good corrosion resistance, which was further supported by a newly formed surface layer of oxides, which, among other things, contributed to an increase in microhardness.

Higher temperatures contributed to obtaining a thicker surface layer for the same length of oxidation, whichindicates an increase in the rate of oxidation. This fact confirms the importance of temperature during thermalprocessing, as a determining factor in the rate of oxidation. At the same time, however, it is necessary to take into accountthat acceleration of oxidation due to higher temperatures can bring the entire newly formed layer tometastable state due to internal and warm effects. The creation of such a structureit allows oxidation in an uncontrolled manner.

On the basis of the experiment carried out, it is possible to come to the conclusion and give the assumption that a further increase in temperature during heat treatment will cause an increase in both microhardness and other mechanical properties (strength, hardness, etc.).

Acknowledgement

This article was supported by SGS UJEP-SGS-2021-48-002-3.

References

[1] PRYMAK, O., BOGDANSKI, D., KÖLLER, M., ESENWEIN, S., & col. (2005). Morphological characterization and in vitro biocompatibility of a porous nickel–titanium alloy. *Biomaterials*, Vol. 26, Issue 29, pp. 5801-5807. ISSN 0142-9612.

[2] BROOKSHIRE, F. V. G., NAGY, W. W., DHURU, V. B., ZIEBERT, G. J., CHADA, S. (1997). *The qualitative effects of various types of hygiene instrumentation on commercially pure titanium and titanium alloy implant abutments: an in vitro and scanning electron microscope study.*

[3] LEYENS, C., PETERS, M. (2003). *Titanium and titanium alloys, Fundamental and applications*. WILEY-VCH, pp. 333-350, 401-404. ISBN: 9783527602117.

[4] KUSMIERCZAK S., SRB R. Influence of Thermomechanical Processing Parameters on Selected Properties of B-post Made of 22MnB5 Steel. *Manufacturing Technology*. 2023;23(6):837-845. doi: 10.21062/mft.2023.105.

[5] XIAOGUANG, F., QI, L., ANMING, Z., YUGUO, S., WENJIA M. (2017). The Effect of Initial Structure on Phase Transformation in Continuous Heating of a TA15 Titanium Alloy. *Metals*, Vol. 7, No. 6, pp. 1-12. ISSN 2075-4701.

[6] PEDERSON, R., BABUSHKIN O., SKYSTEDT F. AND WARREN R. (2003). Use of High Temperature X-ray Diffractometry to Study Phase Transitions and Thermal Expansion Properties in Ti – 6Al – 4V. *Materials Science and Technology*, Vol.19, No. 11, pp. 1533-1538.

[7] LEE, K., YANG, S., YANG, J. (2017) Optimization of Heat-treatment Parameters in Hardening of Titanium Alloy Ti-6Al-4V by using the Taguchi Method. International Journal of Advanced *Manufacturing and Technology*, Vol. 90, pp. 753-761.

[8] HUA, Q., WEIDONG, L. (2011) Theoretical Calculation of β Transition Temperature of Ti-6Al-4V from Valence Electron Level. *Advanced Materials Research*, pp. 299-300, ISSN: 1662-8985.

[9] FIDAN, S., AVCU, E., KARAKULAK, E., YAMANOGLU, R., ZEREN M., SINMAZCELIK T. (2013). Effect of Heat Treatment on Erosive Wear Behaviour of Ti6Al4V alloy. *Materials Science and Technology*, Vol. 29, No. 9, pp. 1088-1094.

[10] IMAM, M. A., GILMORE, C. M., (1983) Fatigue and Microstructural Properties of Quenched Ti-6AI-4V. *Metallurgical Transactions A*, Vol. 14, pp. 223-240.

[11] SUDHAGARA, R. S., JITHIN, V., GEETHA, M., NAGESWARA R. M. (2018). Processing of Beta Titanium Alloys for Aerospace and Biomedical Applications. Titanium Alloys – Novel Aspects of Their Manufacturing and Processing Intech, *Open* 1-18.

[12] HADKE, S., KHATIRKAR, R. K., SHEKHAWAT, S. K., JAIN, S., SAPATE, S. G. (2015) Microstructure Evolution and Abrasive Wear Behavior of Ti-6Al-4V Alloy. *Journal of Materials Engineering and Performance*, Vol. 24, pp. 3969-3981.

[13] SEMIATIN, S. L., KNISLEY, S. L., FAGIN, P. N., ZHANG, F., BARKER D. R. (2003). Microstructure Evolution during Alpha-Beta Heat Treatment of Ti-6Al-4V. *Metallurgical and Materials Transactions A*, Vol. 34, pp. 2377-2386.

[14] QU, S. G., SUN, F. J., YUAN, Z. M., LI, G., LI Q. (2015). Effect of Annealing Treatment on Microstructure and Mechanical Properties of Hot Isostatic Pressing Compacts Fabricated using Ti–6Al–4V Powder. *Powder Metallurgy*, Vol. 58, No. 4, pp. 312-319.

[15] JOVANOVIC, M. T., TADIĆ, S., ZEC S., MIŠKOVIC, Z., BOBIĆ I. (2006). The Effect of Annealing Temperatures and Cooling Rates on Microstructure and Mechanical Properties of Investment Cast Ti–6Al–4V Alloy. *Materials and Design*, Vol. 27, No. 3, pp. 192-199. ISSN 0261-3069.

[16] RAJAGOPAL, K. P. A., JOSE, A. M., SOMAN, A., DCRUZ, C. J., NIVED, S. N., SYAMRAJ, S., VIMALKUMAR P. (2015). Investigation of Physical and Mechanical Properties of Ti Alloy (Ti-6Al-4V) Under Precisely Controlled Heat Treatment Processes. *International Journal of Mechanical Engineering and Technology*, Vol. 6, No. 2, pp. 116-127. ISSN 0976 – 6359.

[17] KLIMAS, J., SZOTA, M., NABIAŁEK, M., ŁUKASZEWICZ, A., BUKOWSKA, A. (2013). Comparative description of structure and properties of Ti6Al4V titanium alloy for biome dical applications produced by two methods: conventional (molding) and innovative (injection) ones, *Journal of Achievements in Materials and Manufacturing Engineering*. Vol. 61, No. 2, pp. 195-201.

[18] GARCIA-ALONSO, M., C., In vitro corrosion behaviour and osteoblast response of thermally oxidised Ti6Al4V alloy, Madrid, *Biomaterials*, 2003.

[19] BLOYCE, A., Surface modification of titanium alloys for combined improvements in corrosion and wear resistance, Birmingham, *Surface and Coatings Technology*, 1999.

[20] MASHEKOVA A., NURTAZAEV A., MASHEKOV S., ALSHYNOVA A., TUSSUPKALIYEVA E. The Influence of the Technological Parameters of Rolling in the Helical Rollers and Longitudinal Wedge Mill on the Quality of Two-Phase Titanium Alloy. *Manufacturing Technology*. 2017;17(3):347-354. doi: 10.21062/ujep/x.2017/a/1213-2489/MT/17/3/347.

[21] HREN I., KUŚMIERCZAK S., HORKÝ R. Use of Electron Microscopy in the Analysis of the Influence of Roughness on the Corrosion Behavior of Selected Ti Alloys. *Manufacturing Technology*. 2023;23(2):161-176. doi: 10.21062/mft.2023.017.

[22] CHEN, J., PAN, C. (2011). Welding of Ti-6Al-4V alloy using dynamically controlled plasma arc welding process. *Transactions of Nonferrous Metals Society of China*, Vol. 21, No. 7, pp. 1506–1512. ISSN 1003-6326.

[23] WU, M., XIN, R., WANG, Y., ZHOU, Y., WANG, K., LIU Q. (2016). Microstructure,

texture and mechanical properties of commercial high-purity thick titanium plates jointed by electron beam welding. *Materials Science and Engineering*, Vol. 677, pp. 50–57.

[24] SQUILLACE, A., PRISCO, U., CILIBERTO, S., ASTARITA, A. (2012). Effect of welding parameters on morphology and mechanical properties of Ti-6Al-4V laser beam welded butt joints. *Journal of Materials Processing Technology,* Vol. 212, pp. 427–436. ISSN 0924-0136.

[25] KASHAEV, N., VENTZKE, V., FOMICHEV, V., FOMIN, F., RIEKEHR. S. (2016). Effect of Nd:YAG laser beam welding on weld morphology and mechanical properties of Ti–6Al–4V butt joints and T-joints. *Optics and Lasers in Engineering*, Vol. 86, pp.172–180.

[26] LI, X., XIE, J., ZHOU, Y. (2005). Effect of oxygen contamination in the argon shielding gas in laser welding of commercially pure titanium thin sheet. *J Mater Sci*, Vol. 40, pp. 3437–3443.

[27] DAI, N., ZHANG, L. C., ZHANG, J., CHEN, Q., WU, M. (2016). Corrosion behavior of selective laser melted Ti-6Al-4 V alloy in NaCl solution. *Corros. Sci.*, Vol. 102, pp. 484-489.

[28] BAI, Y., GAI, X., LI, S., ZHANG, L. C., LIU, Y., HAO, Y., ZHANG, X., YANG, R., GAO, Y. Improved corrosion behaviour of electron beam melted Ti-6Al–4V alloy in phosphate buffered saline. *Corrosion Science*, Vol. 123, pp 289-296. ISSN 0010-938X.

[29] ZIELIŃSKI, A., SOBIESZCZYK, S. (2010). Corrosion of Titanium Biomaterials, Mechanisms, Effects and Modelisation. *Corrosion Reviews*, Vol. 26, pp 1-22.

[30] KOUŘIL, M. (2011). Corrosion rate of construction materials in hot phosphoric acid with the contribution of anodic polarization. Weinheim. *Materials and Corrosion*, Vol. 63, No. 4, pp. 310-316.

[31] KRYSHNA, D. S. R. (2006). Thick rutile layer on titanium for tribological applications. *Tribology International,* Vol. 40, No. 2, pp 329-334. Singapore. ISSN 0301-679X.

[32] ČSN ISO 8407: *Koroze kovů a slitin, Odstraňování korozních zplodin ze vzorků podrobených korozním zkouškám*. Leden 1995. Praha: Český normalizační institut, 1995,12 s.

[33] ČSN 03 8212: *Zabezpečování jakosti korozních zkoušek v umělých atmosférách*. Praha: Český normalizační institut, 1994.

[34] KRYSHNA, D., S., R., Thick rutile layer on titanium for tribological applications, Singapore, *Tribology International,* 2006.

[35] VELTEN, D., *Preparation of TiO_2 layers on CP-Ti and Ti6Al4V by thermal and anodic axidation and by sol-gel coating techniquest and their characterization, Saarbücken*, Wiley Online Library, 2001.